

High-Temperature Reaction Calorimeter

Enthalpy of Formation of Iron Selenides and Nickel Selenides at 1050 K

FREDRIK GRØNVOLD

Kjemisk Institutt A, Universitetet i Oslo, Blindern, Oslo 3, Norway

A calorimeter for measurements of the enthalpy of formation of iron selenides and nickel selenides at about 1050 K is described. Selenium is sealed into a high-melting glass tube, which is placed into a 10 mm diameter quartz tube, open at the top. This tube is put into a larger quartz tube containing the iron or nickel, which is then evacuated and sealed and placed in the calorimeter. The calorimeter and surrounding shields are heated electrically in a tube furnace, and when the temperature approaches 1050 K adjustments are made so that the temperature drift of the calorimeter becomes less than 0.01 K min⁻¹. After an hour or two the selenium container develops a hole and the reaction takes place. The calorimeter, with energy equivalent of about 4 kJ K⁻¹, is operated with isothermal shields and the maximum temperature rise is about 1 K for 1/20 mol Me_{1-x}Se_x. The system is calibrated electrically and the enthalpy of formation within the homogeneity ranges of the Me_{1-x}Se-phases with NiAs-like structures is obtained with a precision of about 0.5 %. For the Fe_{1-x}Se-phase the enthalpy of formation from solid iron and liquid selenium at 1050 K is -34.6 kJ mol⁻¹ at the composition Fe_{0.50}Se_{0.50}. The minimum in enthalpy of formation occurs at the composition Fe_{0.47}Se_{0.53}, where $\Delta H_f = -35.3$ kJ mol⁻¹, while for the composition Fe_{0.429}Se_{0.571} (1/7 Fe₃Se₄) $\Delta H_f = -33.5$ kJ mol⁻¹. The derived standard enthalpy of formation at 298 K for 1/2.04 Fe_{1.04}Se, 1/15 Fe₇Se₈, and 1/7 Fe₃Se₄ is -34.1, -30.9, and -30.3 kJ mol⁻¹, respectively. For the Ni_{1-x}Se-phase the enthalpy of formation from solid nickel and liquid selenium at 1050 K is -40.9, -41.3, and -41.0 kJ mol⁻¹ for the compositions Ni_{0.477}Se_{0.523} (1/39 Ni₁₉Se₂₀), Ni_{0.467}Se_{0.533} (1/15 Ni₇Se₈), and Ni_{0.444}Se_{0.556} (1/9 Ni₄Se₅), respectively. The derived standard enthalpy of formation at 298 K is -36.5, -37.2, and -36.8 kJ mol⁻¹ for the same three compositions.

In studies of transition metal chalcogenides and pnictides knowledge of their thermochemical properties are of fundamental importance. The phases in question often have wide homogeneity ranges at higher temperatures, and in case of the selenides for example, virtually no reliable information

about integral or partial quantities as function of composition is available. A high-temperature reaction calorimeter has therefore been constructed and the enthalpies of formation of iron selenides and nickel selenides have been determined. The calorimeter is equally applicable to studies of arsenides and also of sulfides, phosphides, and other compounds when suitable containers for the volatile component are chosen.

Measurements of reaction enthalpies at elevated temperatures by direct combination of the elements in question offer distinct advantages over aqueous solution calorimetry, since the results in the latter case are obtained as small differences between measurements on combined and uncombined elements. Conditions must be found, however, under which the reaction can go to completion within a relatively short time. In case of the elements under consideration here, the metals must be present in rather finely divided form in order to react quantitatively with selenium in the course of a few minutes at 1050 K. The vapour pressure of elemental selenium is about 3 atm at this temperature and thus causes problems with regard to confinement.

A noteworthy contribution to high temperature reaction calorimetry was made by Kubaschewski and Walter.¹ Their method was extended to comprise a volatile component by Weibke and Schrag² who determined the enthalpies of formation of lower phosphides of iron, cobalt, nickel, and copper with experimental error of about 2.5 %. A pelletized mixture of finely divided metal and phosphorus was sealed into a quartz container and dropped into an adiabatic shield type calorimeter operating around 900 K. The sample mixture was preheated to about 600 K in order that the enthalpy increment for heating the sample mixture and container should largely compensate the enthalpy of reaction. The metal solvent type calorimeters represent a related line of development in which the uncombined and combined elements are dissolved in liquid tin for example, either simultaneously in the compartments of a twin-cell calorimeter, or at different times in a single-cell instrument. The progress in these fields has been surveyed by several authors.³⁻⁵ In the present case no special advantage was seen in the high-temperature solution-type calorimeters, since the major problem was confinement of the selenium gas and not lack of reaction between selenium and the metals.

Dropping of a mixture of the elements into the calorimeter, as was done by Weibke and Schrag,² was not considered precise enough for delineating the enthalpy of formation as a function of composition within the homogeneity range of the solid selenides in question. Thus, for a $\text{Me}_{0.5-\delta}\text{Se}_{0.5+\delta}$ -phase with enthalpy of formation $\Delta H_f^\circ \approx -40 \text{ kJ mol}^{-1}$ and $\delta_{\text{max}} \approx 0.1$ a precision better than 0.5 % might be needed for comparison with theoretical models and meaningful derivation of partial quantities. It was therefore decided that the components should be enclosed in the calorimeter in accurately known amounts, and not introduced by dropping or any other method that would influence the heat exchange parameters of the calorimetric system and also cause uncertainty about the thermodynamic states of the components.

The available enthalpy of formation data for iron selenides refer to the composition FeSe, which according to our earlier investigations⁶⁻⁸ is a two-phase preparation below 457.6°C. It consists of the phases $\text{Fe}_{1.04}\text{Se}$ with tetragonal structure of PbO-like type, and Fe_7Se_8 with hexagonal structure

of NiAs-like type. The only ΔH_f determination performed until 1950 was that by Fabre,⁹ who dissolved FeSe and the uncombined elements in a bromine-water mixture. His results have been reevaluated by several compilers of thermodynamic data. More recently Kapustinskii and Golutvin¹⁰ determined the same quantity by reacting the elements in a bomb calorimeter and correcting for uncombined selenium by their "limiting heat" method.¹¹

Nickel monoselenide is non-stoichiometric in its hexagonal NiAs-like form at 450 and 300°C¹² when prepared from the elements, but is also reported to exist with Millerite-type structure.^{13,14} There are indications that this low-temperature phase contains excess nickel corresponding to the composition Ni₂₁Se₂₀.¹⁵ The only available information about the enthalpy of formation of NiSe stems from Fabre's⁹ solution calorimetric experiments which also have been reevaluated by several authors. The variation in enthalpy of formation within the homogeneity range of the non-stoichiometric Me_{1-x}Se-phase, which is the subject of the present investigation, has not been considered earlier, except in a preliminary study by the author.¹⁶ The thermochemical results obtained here will be integrated with earlier published data on the thermo-physical properties of three iron selenides^{7,8} and three nickel selenides^{17,18} in a forthcoming paper on the thermodynamics of non-stoichiometric iron selenides and nickel selenides with NiAs-like structures.¹⁹

DESIGN AND OPERATION OF THE CALORIMETER

A. Mechanical construction. The calorimeter proper (see Fig. 1) is a cylinder of stainless steel (Uddeholm Stainless 25 with 23.5 % Cr, 21.5 % Ni, 0.07 % C, balance Fe). It is 90 mm in diameter and 170 mm high with a wall thickness of 15 mm. The outside of the calorimeter is completely covered with 0.2 mm silver sheets. The calorimeter has a removable bottom, fastened with three screws. Inside the stainless steel cylinder is cast a 15 mm thick silver wall. A 10 mm thick cylindrical silver disc serves as bottom for the reaction space. The calorimeter body consists of about 5 kg stainless steel and 3 kg silver. The calorimeter is suspended from a lid of stainless steel, and also rests on a ring spacer of fused quartz in order to diminish the strain on the hooks and the lid.

The construction of the reaction vessel offered several difficulties. Both mechanical and electromagnetic devices were tried for breaking the quartz ampoule containing the selenium inside the vessel at high temperatures, but they were not entirely successful. It was found, however, that if selenium were sealed into a Pyrex 1720 glass tube and heated *in vacuo* to about 1050 K, the tube would expand slowly and develop a hole through which the selenium gas could escape and react with the metal. In order to control the expansion of the Pyrex tube better it was put into a slightly larger diameter quartz tube, open at one end. Under these conditions the tube would always blow after being kept at 1050 K for a few hours.

The shield consists of a cylindrical crucible with plane bottom and lid made of stainless steel (Uddeholm Stainless 25). The crucible is 200 mm high, has an internal diameter of 100 mm and a wall thickness of 1 mm. The inside of the crucible is covered with a 0.5 mm silver sheet. To measure the temperature of the shield, three Pt-90Pt10Rh thermocouples are located in the wall of the cylindrical crucible, one at the middle, one 80 mm above, and one 80 mm below the middle at 120° angle. The crucible is attached to a set of five cylindrical radiation shields 1 mm thick and of 120 mm diameter, with 20 mm long spacers of 2 mm stainless steel. The radiation shields rest on tight fitting cylindrical firebricks (Borgestad 07 Porös). Five radiation shields are also fastened to the lid and covered with firebricks. The calorimeter proper with lid, radiation shields and firebricks can be hoisted out of the furnace by means of a rope and pulley.

The same thermostat was used as for the heat capacity measurements.²⁰ It can be described as a large vertical tube furnace. The porcelain (Pythagoras) tube is 1 m long,

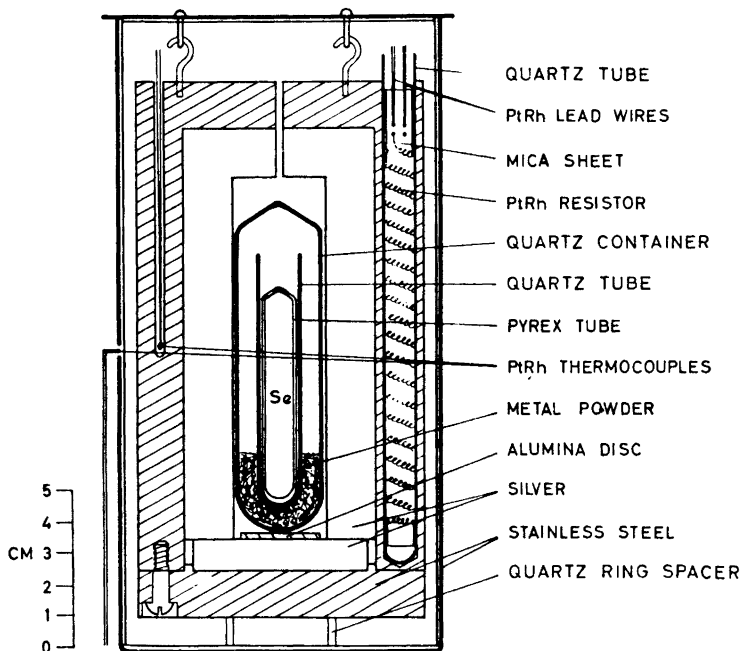


Fig. 1. Reaction calorimeter.

145 mm in outside diameter and is mounted in a 400 mm diameter casing filled with expanded mica (Vermiculite). The heater element (7×0.7 mm² Kanthal A strip) is wound bifilarly on the tube, and the energy supplied through a saturable inductor, which allows the input to the thermostat to vary between 50 and 2500 W.

B. Measuring and control circuits. The temperature sensing element is of platinum wire, 0.2 mm diameter and 8 m long, with a resistance of about 25Ω at room temperature. It was wound non-inductively around a flat mica plate, $400 \times 20 \times 0.2$ mm³, covered with mica plates and bent around the furnace core at the middle and was in as good thermal contact with the heater as possible.

This resistance thermometer constitutes one of the arms in a Wheatstone bridge circuit as indicated in Fig. 2. There are in addition two 100Ω resistors and a 100Ω decade resistor with steps of 0.01Ω to match the platinum resistor. The bridge is energized from a 400 cycles oscillator and the unbalance is amplified electronically and governs the current going through the saturable inductor. In the initial experiments the drift in temperature with time was of the order of 0.01 K per half hour, but after thermostating the room the drift was reduced to about 0.003 K per half hour.

A heating period of about 10 h is needed to bring the calorimeter up to the temperature at which the tube with selenium is about to blow open, and adjustments are made so that the temperature increase is then not more than 0.01 K/min. After an additional hour or two during which temperature measurements are carried out every 30 to 60 sec, the combination of selenium with the metal suddenly takes place. The temperature increases rapidly during a few minutes and then proceeds towards the limiting value, and the measurements are discontinued after about another hour.

The temperature of the calorimeter and the temperature gradients are measured by means of three thermocouples located in the top, middle and the bottom of the calorimeter. The thermocouples are made from 0.5 mm diameter Pt and 90Pt10Rh wires and

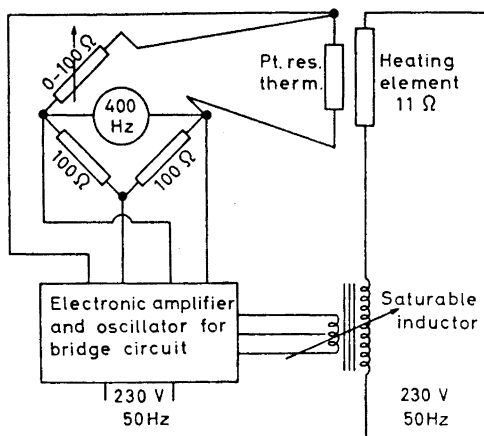


Fig. 2. Thermostat control circuit.

they extend right into the ice reference bath without use of compensating leads. The EMF of the thermocouples is determined by a microvolt potentiometer with five decades (Wolff Kompensator), a set of calibrated standard cells and a mirror galvanometer (Kipp & Zonen A15). In the present setup the scale-value is $0.03 \mu\text{V}/\text{mm}$, which permits reading of the temperatures to 0.01 K. In order to calibrate the thermocouples, their EMF was compared at various temperatures with that of standard thermocouples calibrated at the U.S. National Bureau of Standards at the freezing points of zinc, antimony, silver, and gold.

The temperature increase of about 1 K during the reaction needs to be known to 0.001 K or better and is measured by means of a resistance thermometer. The thermometer is located in a 11 mm diameter hole in the calorimeter wall, about 150 mm deep. The resistor originally consisted of a spiral of 0.2 mm diameter platinum wire about 8 m long and having a resistance of about 25Ω at room temperature, bifilarly wound on a mica frame and put into a silica tube. The tube was closed in the upper end with alumina cement. It turned out, however, that the resistor did not have the required stability when subjected to temperatures above 1000 K and it was therefore soon replaced by a Pt-90Pt10Rh resistor which has shown an excellent stability. This could not be done without loss in sensitivity, as the resistance change per kelvin of the 90Pt10Rh wire is only about 60 % of that of pure platinum at 1050 K.

Outside the calorimeter, the 90Pt10Rh wires were extended by copper wires and connected to a Mueller Bridge (Rubicon Model 1551) for measuring resistances up to 141.1110 abs. Ω in steps of 0.0001Ω . A current of 4.5 mA was continuously running through the PtRh resistor during the measurements, and a deflection corresponding to $0.00003 \Omega \text{ mm}^{-1}$ was observed on the mirror galvanometer (Kipp & Zonen, A15) when the external resistance was 100Ω , so that temperature differences could be read to $\pm 0.0002 \text{ K}$ at 1050 K.

C. Evaluation of the calorimetric data. Calorimetric experiments of the type considered here are ordinarily divided into three periods: (1) an initial period, during which the temperature change of the calorimeter is due entirely to heat transfer between calorimeter and surroundings (thermal leakage); (2) a main period, in which a sufficiently large part of the temperature rise caused by the reaction, or by input of electrical energy, is completed; and (3) a final period in which the temperature change of the calorimeter is considered to be due to thermal leakage only.

The relation between temperature, T , of the calorimeter, and time, t , in an experiment where an exothermic reaction takes place in the calorimeter, is illustrated in Fig. 3. Here the parts AB, BDF, and FG of the curve represent the temperature-time relations

in the initial, main and final periods, respectively. The horizontal line shows the convergence temperature T_∞ of the calorimeter, that is the temperature attained by the calorimeter after an infinite time if the temperature and other properties of the thermostat and further surroundings remain constant.

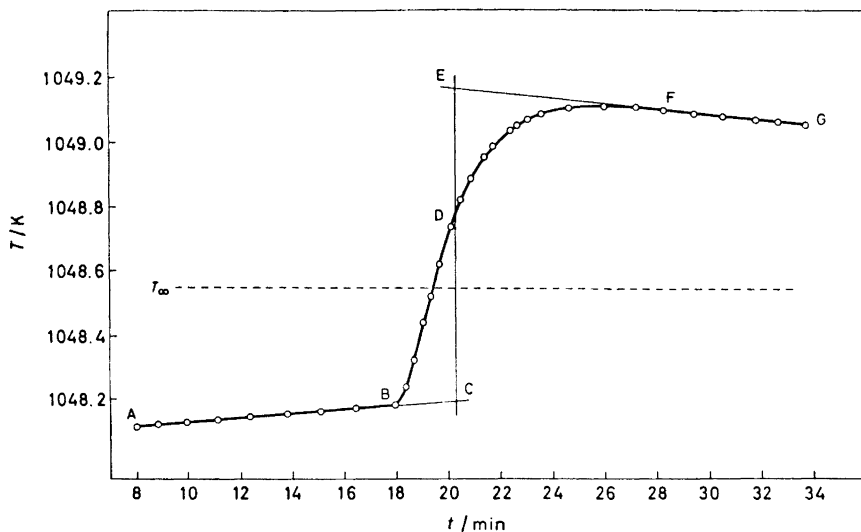


Fig. 3. Temperature-time plot of reaction experiment.

If one lets T_B and T_F denote the temperature of the calorimeter at the beginning and end of the main period, the observed temperature rise may be taken as $T_F - T_B$. This must be corrected for thermal leakage ΔT_1 in order to obtain the corrected temperature rise. The total heat effect ΔQ during the calorimetric experiment can thus be expressed as

$$\Delta Q = \int_{T_B}^{T_E} \varepsilon dT + \int_{t_B}^{t_E} K(T_\infty - T_C) dt$$

where ε is the energy equivalent (or heat capacity) of the calorimeter, K is the heat flow rate coefficient ($E T^{-1} t^{-1}$), T_∞ and T_C are the uniform surface temperatures of the shield and the calorimeter, respectively, and t is the time. In case the system satisfies Newton's law of cooling and its heat capacity, emissivity, and other relevant properties remain constant, then $K/\varepsilon = k$, k being the heat leak modulus (t^{-1}).

As stressed by King and Grover²¹ and more recently by MacLeod,²² deviations from pure Newtonian cooling obtain in the final period when the hot body—or the electrical heater for that matter—is in poor thermal contact with the calorimeter body. Under such conditions, or when the energy release from the sample is partially delayed due to transformations, the heat supplied to the calorimeter might not be neglected after a certain time, and the correction procedure has to be changed accordingly.

In the absence of such complications, or when an accuracy of not more than 0.2 % is sought, various correction methods are equally well applicable. The correction for thermal leakage might then be evaluated directly from the above equation after evaluating k and T from the experimental data. This has been done graphically here (see Fig. 4) by plotting the logarithm of $|R - R_\infty|$ as function of time for the initial and final periods, R_∞ being chosen as to give the best straight line relationship for both periods.

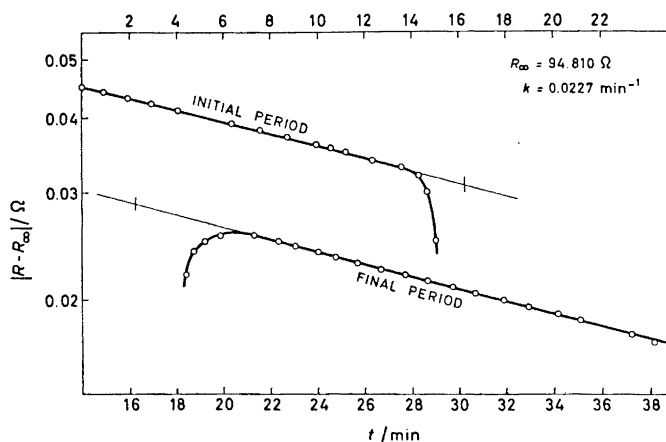


Fig. 4. Semi-logarithmic plot of calibration experiment.

The need for estimating a completion time for the main period is not present in the method of Dickinson.²³ His method of finding the corrected temperature rise consists in extrapolating the rating curves AB and FG, (*cf.* Fig. 3) to a time t_x at which the two areas BCD and DEF are equal. The temperature difference, $T_E - T_C$, obtained in this way is the corrected temperature rise. Instead of finding the time t_x by graphical integration, Dickinson showed that it can be found algebraically with sufficient accuracy from a simplified analysis of the heat leakage problem, as the time when the temperature has reached 63 % of its final value. A large number of observations by Dickinson gave $t_x = 0.57$ to 0.62 , *i.e.* slightly less than predicted, probably due to the fact that the temperature rise does not begin as soon as required by the assumptions.

D. *Determinations of the energy equivalent of the calorimeter.* By determining the corrected temperature rise ΔT of the calorimeter for a known energy input ΔQ , the energy equivalent ε of the calorimeter is found as

$$\varepsilon = \Delta Q / \Delta T$$

The change in internal energy ΔE for a reaction occurring at constant volume, or enthalpy ΔH for a reaction at constant pressure, can then be expressed as a product of the corrected temperature rise and the energy equivalent of the calorimeter.

There are three methods commonly used for evolving energy in a calorimetric system for calibration purposes: (1) transforming a measured quantity of electrical energy into heat; (2) letting a chemical reaction (with heat of reaction already determined accurately) take place in the calorimeter; (3) introducing a substance of known heat capacity and temperature into the calorimeter. Method 1 is most directly related to the energy unit and has been used here. The quantity of energy supplied to the calorimeter is measured as a product of the potential drop across the heating coil, the current running through it, and time. In the actual calibration experiments a Nichrome resistor of about 12.0Ω (24.70 g 80Ni 20Cr wire and 54.92 g vitreous quartz) was put into the calorimeter instead of the reaction vessel. Current and potential leads were connected to the resistor right outside the calorimeter vessel and connected to the measuring circuit and energy supply as shown in Fig. 5.

The energy is taken from a 96 V storage battery and a 35Ω adjustable resistor is put in series with the heater. A 0.01Ω standard resistor ($0.010\,000$, abs. Ω at 25°C) serves for determining the current by means of a microvolt potentiometer (Wolff Kompensator). The time of energy input is measured accurately by a frequency counter (Beckman Model 5571) shunted to the heater.

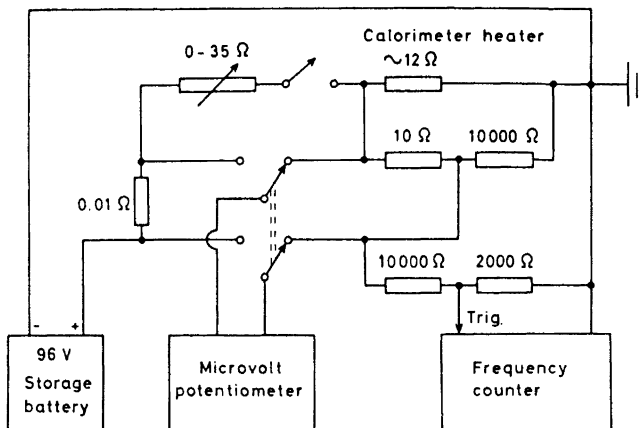


Fig. 5. Energy input circuit diagram.

The results of a series of calibration experiments are presented in Table 1. The energy inputs varied between about 3.0 and 4.5 kJ and the temperature of beginning energy input (T_B) was about 1050 K each time. The asymptotic temperature of the calorimeter (T_∞) and the corrected temperature rise are also given in the table. The latter was obtained using Dickinson's method of calculation (D), with a mean time corresponding to 60 % of the total temperature rise, and the Regnault-Pfaundler method (RP). The resulting mean value for the energy equivalent of the calorimeter at 1050 K is 3860.4 JK^{-1} with a standard deviation of 10.1 JK^{-1} . Slightly different values have been obtained in later calibrations due to changes in the construction of the calorimeter. Several earlier experiments¹⁶ in which the energy inputs were more uncertain resulted in a considerably larger spread ($\sigma = 33 \text{ JK}^{-1}$) and are regarded as superceded by the newer data.

From the observed energy equivalent and knowledge about the heat capacity of silver ($0.2815 \text{ J g}^{-1}\text{K}^{-1}$ at 1050 K according to Hultgren *et al.*²⁴) and additional materials in the calorimeter ($\sim 10 \text{ g Pt}$, $9 \text{ g Al}_2\text{O}_3$, and 12 g SiO_2) the heat capacity of the stainless steel becomes $0.591 \text{ J g}^{-1}\text{K}^{-1}$ at 1050 K. This value might be compared with $0.586 \text{ J g}^{-1}\text{K}^{-1}$

Table 1. Calibration data for the reaction calorimeter.

Input/J	T_B/K	T_∞/K	$\Delta T_D/\text{K}$	$\Delta T_{RP}/\text{K}$	Energy equiv. ϵ/JK^{-1}
4039.8	1050.1	1049.8	1.024	1.030	3934
4010.3	1049.9	1050.2	1.013	1.008	3969
3993.9	1051.0	1051.5	1.019	1.020	3918
4139.3	1050.9	1051.5	1.052	1.058	3924
3734.8	1050.8	1051.0	0.945	0.948	3946
4335.9	1051.1	1051.5	1.100	1.104	3935
4769.4	1051.1	1051.6	1.201	1.206	3963
3159.4	1051.1	1051.4	0.804	0.807	3922
				Mean value	3938.9
				- Heater	78.5
				Empty calorimeter	3860.4

$\text{g}^{-1} \text{K}^{-1}$ reported by Pallister²⁵ for an iron-nickel steel with 28.37 % Ni, and the values $0.619 \text{ J g}^{-1} \text{K}^{-1}$ by Douglas and Dever²⁶ for a steel with 18.3 % Cr, 11.1 % Ni, 1.30 % Mn, 0.86 % Nb, 0.52 % Si, 0.08 % C, balance iron.

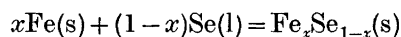
RESULTS AND DISCUSSION

A. Iron selenides. At 1050 K the Fe_{1-x}Se -phase is the only intermediate solid phase in the iron selenium system,^{27,28} and the enthalpy of formation determinations have primarily been carried out for this phase. Only $\text{FeSe}_{0.90}$, $\text{FeSe}_{0.95}$, $\text{FeSe}_{1.40}$, and $\text{FeSe}_{1.50}$ are two-phase samples; the remaining belong to the Fe_{1-x}Se -phase with NiAs-like structure and vacant metal atom sites. In the experiments iron powder was used. It was prepared from iron(III) oxide (*Ferrum oxydatum p.a.*, Merck) by reduction with dry, purified hydrogen gas at 700°C until constant mass was attained. According to a spectrographic analysis the impurities were ~ 100 ppm Ni, ~ 100 ppm Si, and ~ 10 ppm Mn. The selenium used was a high-purity material from Bolidens Gruvaktiebolag containing only 2 ppm Cl, 0.8 ppm Fe, 0.3 ppm K, 0.4 ppm Na and 12 ppm non-volatile matter as impurities. In Table 2 the experimental data are given

Table 2. Enthalpy of formation data for iron selenides for 1 mol of mixture.

Composition	Fe/g	Se/g	$T_{\text{B}}/^\circ\text{C}$	$T_{\infty}/^\circ\text{C}$	$\Delta T_{\text{c}}/\text{K}$	$\varepsilon/\text{kJ K}^{-1}$	$\Delta H_{\text{f}}/\text{kJ mol}^{-1}$
$\text{FeSe}_{0.90}$	2.940	3.740	775.3	775.7	0.851	3.910	-33.04
$\text{FeSe}_{0.95}$	2.864	3.847	776.2	776.4	0.864	3.919	-34.11
			776.7	777.1	0.862	3.910	-33.95
$\text{FeSe}_{1.00}$	2.793	3.948	774.7	775.2	0.883	3.922	-34.48
			775.6	776.5	0.891	3.915	-34.66
$\text{FeSe}_{1.05}$	2.724	4.044	776.3	777.7	0.896	3.915	-34.83
$\text{FeSe}_{1.10}$	2.660	4.136	775.5	777.1	0.906	3.912	-35.19
$\text{FeSe}_{1.15}$	2.598	4.224	777.4	777.8	0.902	3.917	-35.08
			777.8	778.0	0.913	3.907	-35.42
$\text{FeSe}_{1.20}$	2.539	4.307	772.5	773.2	0.892	3.922	-34.73
$\text{FeSe}_{1.25}$	2.482	4.387	775.6	776.1	0.880	3.917	-34.24
$\text{FeSe}_{1.30}$	2.428	4.463	775.9	777.6	0.868	3.906	-33.68
$\text{FeSe}_{1.35}$	2.377	4.536	777.4	777.8	0.863	3.918	-33.61
			774.7	775.6	0.860	3.914	-33.46
$\text{FeSe}_{1.40}$	2.327	4.606	776.4	776.9	0.832	3.916	-32.41
			777.0	777.4	0.831	3.906	-32.64
$\text{FeSe}_{1.50}$	2.234	4.734	775.9	777.9	0.807	3.905	-31.35

for selenides of different composition. These include the masses of iron and selenium used, the temperature at which the tube with selenium bursted (T_{B}), the convergence temperature of the calorimeter (T_{∞}), the corrected temperature rise (ΔT_{c}), the energy equivalent of the loaded calorimeter (ε), and the derived enthalpy of formation values for the reaction



In order to arrive at values for the enthalpy of formation of the selenides from the solid metal and liquid selenium under its vapour pressure at 1050 K,

the results have to be corrected for complete or partial condensation of the selenium vapour present. The tubes containing the selenium have a vapour space of about 5 cm³ when they blow. The volume was estimated within ± 0.2 cm³ by observation of the tube after completion of the reaction. For the iron-rich selenides the partial pressure of selenium over the samples is negligible, and the condensation correction (for the 0.1 mol of mixture) is +4.9 J cm⁻³ according to the results by Bonilla and Shulman.²⁹ Svendsen³⁰ has measured the selenium pressure over the selenides. It increases from 7.8 cmHg for FeSe_{1.25} to about 40 cmHg for FeSe_{1.50}, and the enthalpy of evaporation of selenium into the ~ 50 cm³ volume of the reaction chamber changes correspondingly from about -1 J to -5 J.

An estimate of the standard deviation in the measurements might be obtained from the deviations of the individual measurements from the derived curve, and also taking the uncertainty in the electrical calibration into account. In this way the precision is estimated to be 0.6 %. A possible source of error in the present measurements is incomplete or delayed reaction. The calorimeter was constructed such that it only took a few minutes to open it for inspection of the reaction vessel to see if any unreacted selenium were left. This was only found to be the case for FeSe_{1.40} and FeSe_{1.50}, in accordance with the fact already known from X-ray studies that they should be two-phase products consisting of FeSe_{1.35} and selenium. Even though all of the selenium had reacted with iron there was still the possibility that the composition of the selenide varied in different parts of the reaction vessel. X-Ray powder photographs were therefore taken and compared with those of other samples that had surely reached equilibrium at the same temperature. The photographs were fully concordant and – although not showing as sharp lines as those of tempered specimens – confirmed that the reactions had gone to completion.

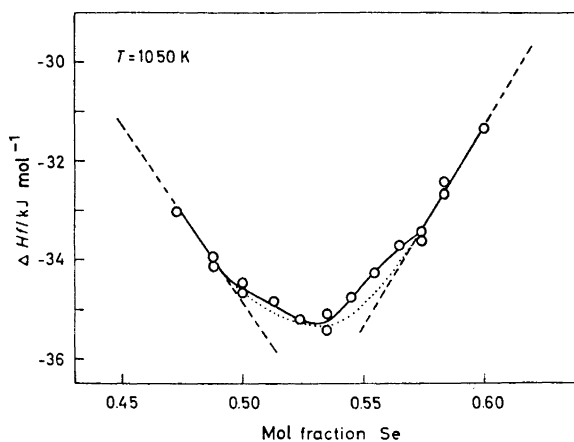


Fig. 6. Enthalpy of formation for 1 mol Fe_{1-x}Se_x at 1050 K. O, represents experimental results; ..., represents equation $\Delta H = x_{Fe}x_{Se}[A_0 + A_1(x_{Se} - x_{Fe}) + A_2(x_{Se} - x_{Fe})^2]$ fitted to the curve at $x_{Se} = 0.50, 0.533, \text{ and } 0.573$.

The enthalpy of formation for 1 mol of $\text{Fe}_{1-x}\text{Se}_x$ mixture is shown in Fig. 6 as function of composition. It changes from $-34.6 \text{ kJ mol}^{-1}$ at the stoichiometric composition $\text{Fe}_{0.50}\text{Se}_{0.50}$ to a minimum value of $-35.3 \text{ kJ mol}^{-1}$ at the composition $\text{Fe}_{0.47}\text{Se}_{0.53}$ ($\text{FeSe}_{1.13}$). From then on it increases again and reaches $-33.5 \text{ kJ mol}^{-1}$ around the composition $\text{Fe}_{0.43}\text{Se}_{0.57}$ ($\text{FeSe}_{1.35}$). The solubility of selenium in iron is less than 0.5 at. % at 1200 K,²³ and the integral enthalpy of formation of the α -Fe-phase with dissolved selenium in equilibrium with the FeSe-phase is thus practically equal to zero. The enthalpy values for $\text{FeSe}_{0.90}$ and $\text{FeSe}_{0.95}$ conform with the presence of a two-phase region up to the latter composition. A change in slope of the enthalpy curve apparently occurs at about $\text{FeSe}_{0.98}$, which therefore marks the iron-rich limit of the FeSe-phase at 1050 K. On the selenium side, terminal solubility of about 0.1 at. % iron is observed by Dutrizac *et al.*³¹ at 800°C. Solution experiments of FeSe_2 in selenium in the region 220 to 585°C by Dutrizac *et al.*³² led to an enthalpy of solution value for FeSe_2 in selenium of only $+4 \text{ kJ mol}^{-1}$. The common tangent of the ΔH -curve for the selenium phase and the FeSe-phase touches the latter close to the composition $\text{FeSe}_{1.35}$ where the data indicate it to bulge outwards. Thus, the enthalpy curve for the FeSe-phase is somewhat irregular, with added stability around the compositions FeSe , Fe_7Se_8 and Fe_3Se_4 . This is apparent when a smooth curve is generated, using the series expansion by Guggenheim³³ for the enthalpy of mixing and limiting it to three terms (*cf.* Fig. 6):

$$\Delta H = x_{\text{Fe}}x_{\text{Se}}[A_0 + A_1(x_{\text{Se}} - x_{\text{Fe}}) + A_2(x_{\text{Se}} - x_{\text{Fe}})^2]$$

To what extent this is due to residual configurational order at 1050 K, suitable binding configurations, or other causes remains to be ascertained.

The present enthalpy of formation results can be accurately transposed to lower temperatures utilizing the earlier heat capacity and enthalpy determinations⁸ in the range 5 to 1050 K for the three iron selenides $\text{Fe}_{0.510}\text{Se}_{0.490}$, $\text{Fe}_{0.467}\text{Se}_{1.533}$, and $\text{Fe}_{0.429}\text{Se}_{0.571}$, which all are single-phase preparations at lower temperatures, and available data for iron³⁴ and selenium.³⁵ The results at 298 K are presented in Table 3. For the two selenium-rich compositions

Table 3. Enthalpy of formation of crystalline iron selenides from α -iron and hexagonal selenium at 298 K.

Composition	$\Delta H_f/\text{kJ mol}^{-1}$	Authors
$\text{Fe}_{0.510}\text{Se}_{0.490}$	-34.1 ± 0.2	Present
$\text{Fe}_{0.467}\text{Se}_{0.533}$	-30.9 ± 0.2	Present
$\text{Fe}_{0.429}\text{Se}_{0.571}$	-30.3 ± 0.2	Present
$\frac{1}{2}\text{FeSe}$	-38.6	Fabre ⁹
$\frac{1}{2}\text{FeSe}$	-27	Bichowsky and Rossini ³⁶
$\frac{1}{2}\text{FeSe}$	-34.5	Rossini <i>et al.</i> ³⁷
$\frac{1}{2}\text{FeSe}$	-37.7 ± 2	Kubaschewski <i>et al.</i> ⁵
$\frac{1}{2}\text{FeSe}$	-37.7 ± 0.6	Kapustinskii and Golutvin ¹⁰

with NiAs-like structures the enthalpies of formation differ only slightly. The low value for $\text{Fe}_{0.510}\text{Se}_{0.490}$ reflects the large decrease in enthalpy on transformation of the hexagonal iron monoselenide (plus excess iron) into the tetragonal phase. Close control of composition and structures is therefore needed in the FeSe-region for meaningful derivation of the enthalpy of formation.

The only iron selenide for which enthalpy of formation data are available in the literature is FeSe. The original solution calorimetric results by Fabre⁹ for crystalline FeSe is given in Table 3 together with later evaluations by Bichowsky and Rossini,³⁶ Rossini *et al.*³⁷ and Kubaschewski *et al.*⁵ All evaluations except that by Bichowsky and Rossini³⁶ indicate higher numerical values for the enthalpy of formation of iron monoselenide than found here. This is also the case with the bomb calorimetric determinations by Kapustinskii and Golutvin,¹⁰ but their results do not seem properly averaged.

B. Nickel selenides. The metal-rich phases in the nickel selenium system were not investigated in detail since they did not form completely within the short time required for obtaining accurate results. Therefore, only nickel monoselenide and compositions richer in selenium will be considered here. According to earlier investigations,¹⁵ $\text{NiSe}_{1.00}$ consists of two solid phases at 1050 K, the $\text{Ni}_{3-x}\text{Se}_2$ -phase with face-centered cubic structure³⁸ and the Ni_{1-x}Se -phase with NiAs-like structure. The composition range of the latter phase presumably extends between $\text{Ni}_{0.98}\text{Se}$ and $\text{Ni}_{0.77}\text{Se}$ at this temperature. At higher selenium contents the NiSe_2 -phase with cubic structure of the pyrite-type appears.

In the experiments finely divided nickel was used. It was prepared by reducing "Nickel oxide, low in cobalt and iron" from the British Drug Houses with hydrogen gas at 650°C until constant mass was attained. The selenium used was the same as for the iron selenides. Experimental data for the different nickel selenides are given in Table 4 together with the derived enthalpy of formation values. The latter include corrections for complete or partial condensation of the selenium in the tubes.

Table 4. Enthalpy of formation data for nickel selenides for 1 mol of mixture.

Composition	Ni/g	Se/g	$T_B/^\circ\text{C}$	$T_F/^\circ\text{C}$	$\Delta T_c/\text{K}$	$\epsilon/\text{kJ K}^{-1}$	$\Delta H_f/\text{kJ mol}^{-1}$
$\text{NiSe}_{1.00}$	2.935	3.948	779.3	778.8	1.029	3.909	-39.97
$\text{NiSe}_{1.05}$	2.862	4.045	775.8	775.8	1.053	3.910	-40.93
$\text{NiSe}_{1.10}$	2.795	4.136	773.3	774.2	1.073	3.908	-41.69
			775.4	775.8	1.060	3.906	-41.16
$\text{NiSe}_{1.15}$	2.729	4.224	776.2	777.3	1.054	3.910	-41.01
			775.9	776.5	1.059	3.912	-41.18
$\text{NiSe}_{1.20}$	2.668	4.307	774.4	777.4	1.060	3.905	-41.14
$\text{NiSe}_{1.30}$	2.552	4.463	775.3	775.6	1.051	3.903	-40.77
$\text{NiSe}_{1.40}$	2.445	4.606	775.8	776.2	1.029	3.905	-39.94
$\text{NiSe}_{1.80}$	2.096	5.076	775.7	776.0	0.901	3.911	-35.01
$\text{NiSe}_{2.00}$	1.956	5.264	778.9	776.1	0.842	3.911	-32.69

In the region $\text{NiSe}_{1.3}$ to NiSe_2 a selenium pressure of 24 cmHg was measured by Svendsen³⁰ at 1050 K. The enthalpy of evaporation of selenium in the reaction chamber is accordingly about -3 J J in the two-phase region $\text{NiSe}_{1.3}$ to $\text{NiSe}_{2.0}$, -2 J for $\text{NiSe}_{1.20}$, and negligible for more nickel-rich selenides.

The enthalpy of formation results for 1 mol of $\text{Ni}_{1-x}\text{Se}_x$ mixture are shown in Fig. 7. They change from $-40.0 \text{ kJ mol}^{-1}$ at the stoichiometric composition

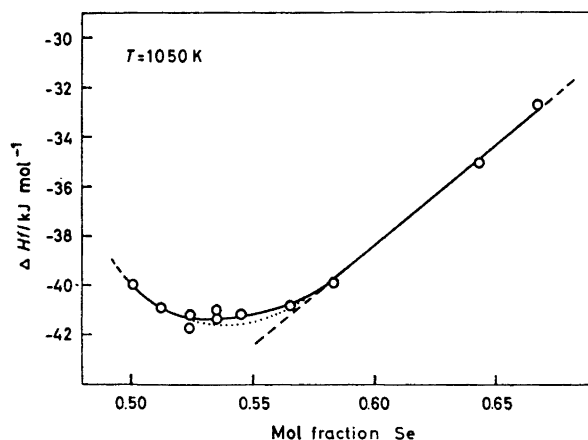


Fig. 7. Enthalpy of formation for 1 mol $\text{Ni}_{1-x}\text{Se}_x$ at 1050 K. ○, represents experimental results; ..., represents equation $\Delta H = x_{\text{Ni}}x_{\text{Se}}[A_0 + A_1(x_{\text{Se}} - x_{\text{Ni}}) + A_2(x_{\text{Se}} - x_{\text{Ni}})^2]$ fitted to the curve at $x_{\text{Se}} = 0.50, 0.533, \text{ and } 0.556$.

$\text{Ni}_{0.50}\text{Se}_{0.50}$ to a minimum of $-41.3 \text{ kJ mol}^{-1}$ at the composition $\text{Ni}_{0.47}\text{Se}_{0.53}$. At the limit of the homogeneity range of the Ni_{1-x}Se -phase the enthalpy of formation approaches $-40.7 \text{ kJ mol}^{-1}$, and reaches $-32.7 \text{ kJ mol}^{-1}$ at the composition $\text{Ni}_{0.33}\text{Se}_{0.67}$ ($\approx \text{NiSe}_2$). In this case a smooth curve through the values for NiSe , $\text{NiSe}_{1.10}$, and $\text{NiSe}_{1.25}$ follows the observed curve for the Ni_{1-x}Se -phase rather closely in the nickel-rich region, but a slight destabilization occurs in the region $\text{NiSe}_{1.15}$ to $\text{NiSe}_{1.20}$.

For the three nickel selenides $\text{Ni}_{0.487}\text{Se}_{0.513}$, $\text{Ni}_{0.467}\text{Se}_{0.533}$ and $\text{Ni}_{0.444}\text{Se}_{0.556}$ the enthalpy of formation below 1050 K can be accurately derived with

Table 5. Enthalpy of formation of crystalline nickel selenides from nickel and hexagonal selenium at 298 K.

Composition	$\Delta H_f/\text{kJ mol}^{-1}$	Authors
$\text{Ni}_{0.487}\text{Se}_{0.513}$	-36.5 ± 0.2	Present
$\text{Ni}_{0.467}\text{Se}_{0.533}$	-37.2 ± 0.2	Present
$\text{Ni}_{0.444}\text{Se}_{0.556}$	-36.8 ± 0.2	Present
$\frac{1}{2}\text{NiSe}$	-38.5	Fabre ⁹
$\frac{1}{2}\text{NiSe}$	-29	Bichowsky and Rossini ³⁶
$\frac{1}{2}\text{NiSe}$	-21 ± 6	Rossini <i>et al.</i> ³⁷

recourse to earlier heat capacity and enthalpy determinations of nickel,²⁴ selenium,³⁵ and the selenides.^{17,18} The values at 298 K are presented in Table 5 together with literature data for NiSe. Within the homogeneity range of the Ni_{1-x}Se-phase the enthalpy of formation is seen to be remarkably constant on 1 mol of atom basis. The original results by Fabre⁹ for NiSe agree much better with the present ones than the revaluations of his measurements by Bichowsky and Rossini³⁶ and Rossini *et al.*³⁷ No further revaluations of these solution calorimetric measurements will be attempted here.

Acknowledgements. The author should like to express his gratitude to *Norges almenvitenskapelige forskningsråd* for continued support. The calorimeter was constructed in the Department workshop under the able direction of Amund Helgesen. The assistance of Torkild Thurmann-Moe and Arvid Hempel with some of the measurements and calculations is recognized with thanks. Sven R. Svendsen kindly made vapor pressure results on the selenides available prior to publication.

REFERENCES

1. Kubaschewski, O. and Walter, A. *Z. Elektrochem.* **45** (1939) 630, 732.
2. Weibke, F. and Schrag, G. *Z. Elektrochem.* **47** (1941) 222.
3. Kubaschewski, O. and Hultgren, R. In Skinner, H. A., Ed., *Experimental Thermochemistry*, Interscience, London and New York 1962, Vol. 2, p. 343.
4. Grønvold, F. *Proc. Symp. Thermodynamics*, July 22–27, 1965, IAEA, Vienna 1966, Vol. 1, p. 35.
5. Kubaschewski, O., Evans, E. Ll. and Alcock, C. B. *Metallurgical Thermochemistry*, 4th Ed., Pergamon, Oxford 1967.
6. Haraldsen, H. and Grønvold, F. *Tidsskr. Kjemi, Bergv. Met.* **10** (1944) 98; *Structure Reports* **9** (1955) 97.
7. Grønvold, F. and Westrum, E. F., Jr. *Acta Chem. Scand.* **13** (1959) 241.
8. Grønvold, F. *Acta Chem. Scand.* **22** (1968) 1219.
9. Fabre, C. *Ann. Chim. Phys.* **10** (1887) 472.
10. Kapustinskii, A. F. and Golutvin, Yu. M. *Zh. Fiz. Khim.* **25** (1951) 729.
11. Kapustinskii, A. F. and Golutvin, Yu. M. *Zh. Fiz. Khim.* **25** (1951) 7.
12. Grønvold, F. and Jacobsen, E. *Acta Chem. Scand.* **10** (1956) 1440.
13. Levi, G. R. and Baroni, A. *Z. Krist.* **92** (1935) 210.
14. Hiller, J.-H. and Wegener, W. *Neues Jahrb. Mineral.* **94** (1960) 1147.
15. Kuznetsov, V. G., Eliseev, A. A., Spak, Z. S., Palkina, K. K., Sokolova, M. A. and Dmitriev, A. V. *Voprosy Met. Fiz.* **1961** 159.
16. Grønvold, F. Paper presented at the *XVI International Congress of IUPAC*, Paris 1957.
17. Grønvold, F., Thurmann-Moe, T., Westrum, E. F., Jr. and Levitin, N. E. *Acta Chem. Scand.* **14** (1960) 634.
18. Grønvold, F. *Acta Chem. Scand.* **24** (1970) 1036.
19. Grønvold, F. *Acta Chem. Scand.* *To be published.*
20. Grønvold, F. *Acta Chem. Scand.* **21** (1967) 1695.
21. King, A. and Grover, H. *J. Appl. Phys.* **12** (1941) 557.
22. MacLeod, A. C. *Trans. Faraday Soc.* **63** (1967) 289.
23. Dickinson, H. C. *Bur. Std. (U.S.) Sci. Pap.* **11** (1914) 189.
24. Hultgren, R., Orr, R. L., Anderson, P. D. and Kelley, K. K. *Selected Values of Thermodynamic Properties of Metals and Alloys*, Wiley, New York 1963.
25. Pallister, P. R. *J. Iron Steel Inst.* **154** (1946) 83P, 90P; **161** (1949) 87.
26. Douglas, T. B. and Dever, J. L. *J. Res. Natl. Bur. Std.* **54** (1955) 15.
27. Tröften, P. and Kullerud, G. *Carnegie Inst. Washington Yearbook* **60** (1961) 175.
28. Kullerud, G. *Carnegie Inst. Washington Yearbook* **67** (1969) 175.
29. Bonilla, C. F. and Shulman, G. *Nucleonics* **22** (1964) 58.

30. Svendsen, S. R. *Personal communication*.
31. Dutrizac, J. E., Janjua, M. B. I. and Toguri, J. M. *Can. J. Chem.* **46** (1968) 1171.
32. Dutrizac, J. E., Janjua, M. B. I. and Toguri, J. M. *Can. Met. Quart.* **7** (1968) 91.
33. Guggenheim, E. A. *Trans. Faraday Soc.* **33** (1937) 151.
34. Orr, R. L. and Chipman, J. *Trans. Met. Soc. AIME* **239** (1967) 630.
35. Grønvold, F. *Unpublished results*.
36. Bichowsky, F. R. and Rossini, F. D. *The Thermochemistry of Chemical Substances*, Reinhold, New York 1936.
37. Rossini, F. D., Wagman, D. D., Evans, W. H., Levine, S. and Jaffe, I. *Selected Values of Chemical Thermodynamic Properties, Natl. Bur. Std. (U.S.) Circ. No. 500*, 1952.
38. Grønvold, F., Møllerud, R. and Røst, E. *Acta Chem. Scand.* **20** (1966) 1997.
39. Grønvold, F. and Westrum, E. F., Jr. *Inorg. Chem.* **1** (1962) 36.

Received June 3, 1971.